Applied Catalysis B: Environment and Energy 352 (2024) 123988

Contents lists available at ScienceDirect

Applied Catalysis B: Environment and Energy

journal homepage: www.elsevier.com/locate/apcatb

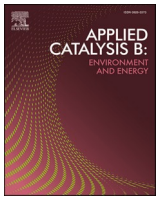

Enhanced catalytic hydrogenolysis of natural rubber to natural gas over Ru/ZrO_2 via phase control strategy

Zhiwen Ren [a,b,1], Xiaoqin Si [c,1], Qian Liu [a], Mengjie Li [a], Hao Chen [a], Rui Lu [a], Hongliang Liang [d], Fang Lu [a,*]

[a] Dalian Institute of Chemical Physics, Chinese Academy of Sciences, Dalian 116023, China
[b] University of Chinese Academy of Sciences, Beijing 100049, China
[c] School of Chemical Engineering, Zhengzhou University, Zhengzhou 450001, China
[d] Yongjiang Laboratory, Ningbo 315202, China

ARTICLE INFO

Keywords:
Rubber wastes
Natural gas
Ru/ZrO_2 catalyst
C=C hydrogenation
C-C cleavage

ABSTRACT

The inert C=C and C-C bonds is a major limitation for the degradation and utilization of rubber wastes, which has resulted in the increasingly serious environmental crisis. Here we developed an efficient strategy to catalyze complete cleavage of C=C and C-C bonds in natural rubber by the enhanced reaction activity of Ru-based catalysts with the modulated ZrO_2 crystal phases. And 95.0% of gas carbon yield with 98.6 mol% of CH_4 and 1.4 mol% of C2-C4 hydrocarbons was achieved over $Ru/m\text{-}ZrO_2$, which was more than 3 times higher than gas carbon yield over $Ru/c\text{-}ZrO_2$ and $Ru/t\text{-}ZrO_2$. The investigation on reaction pathway displayed that the primary hydrogenation of C=C bonds with high bond energy would promote the transformation of natural rubber. The Ru^0 species and spill-over hydrogen in $Ru/m\text{-}ZrO_2$ catalyst acted in synergy for the catalytic hydrogenolysis of natural rubber. Ultimately, various rubber wastes were directly converted to natural gas, it could provide a new perspective for the chemical upcycling of the accumulated rubber wastes.

1. Introduction

Natural rubber as the natural product from rubber plant is an organic polymer of isoprene (polyisoprene $(C_5H_8)_n$) [1–4]. Owing to the unique elasticity, strong corrosion resistance and sustainability, natural rubber has been extensively used in the conventional transportation, medical and hygienic fields [5–8]. With the extended application of the modern rubber industry, more rubber wastes were abandoned to the environment, which was difficult to naturally degrade for the inert C=C and C-C bonds [9,10]. A large amount of rubber wastes would end up by the common disposal means of landfill or incineration [11,12]. However, due to the inertness of chemical bonds in natural rubber, rubber wastes were largely accumulated in environment, which has brought about the increasingly severe pollution problem. Although incineration could utilize the partial energy of rubber wastes, it would also lead to the atmospheric contamination [13,14]. Thus, the development of chemical upcycling strategy has been considered as a relatively more robust and versatile route to dispose of rubber wastes, which could contribute to the sustainable and low-carbon future [15,16].

The chemical bonds involving C=C and C-C bonds ubiquitously exist in the organic polymers [17]. In contrast with the relatively mature strategy for the formation of C=C and C-C bonds, the depolymerization of these chemical bonds urgently needs a great development to resolve the accumulated rubber wastes in ecological environment [16]. In recent decades, the pyrolysis treatments, a commonly used methodology for the thermal degradation of rubber wastes, has been extensively studied in fixed beds, spouted beds and fluidized beds. It is normally performed at 400–900 °C with the high pressure in an inert atmosphere to generate the gas, liquid and solid products [18–20]. However, the high operation temperature would be energy intensive for the inert C=C and C-C bonds cleavage of rubber wastes intrinsic property, and the gas yield was relatively low with the different catalysts, such as nano-ZSM-5/MgAl-LDO, Ni/ZSM-5 and Pd/Hbeta Pd/TiO_2 [21–23]. The catalytic hydrogenation is a promising pathway for the transformation of C=C bonds with the high bond energy, it uses hydrogen and the typical catalysts of $C_4H_6O_4Pd$, $OsHCl(CO)(O_2)(PCy_3)_2$ and $[Ir(cod)(PCy_3)(py)]PF_6$ for the conversion of C=C bonds to C-C bonds in rubber [24–26]. The involved homogeneous catalysts and complex products

* Corresponding author.
E-mail address: lufang@dicp.ac.cn (F. Lu).
[1] *These authors contributed equally to this work.*

https://doi.org/10.1016/j.apcatb.2024.123988
Received 30 December 2023; Received in revised form 11 March 2024; Accepted 19 March 2024
Available online 20 March 2024
0926-3373/© 2024 Elsevier B.V. All rights reserved.

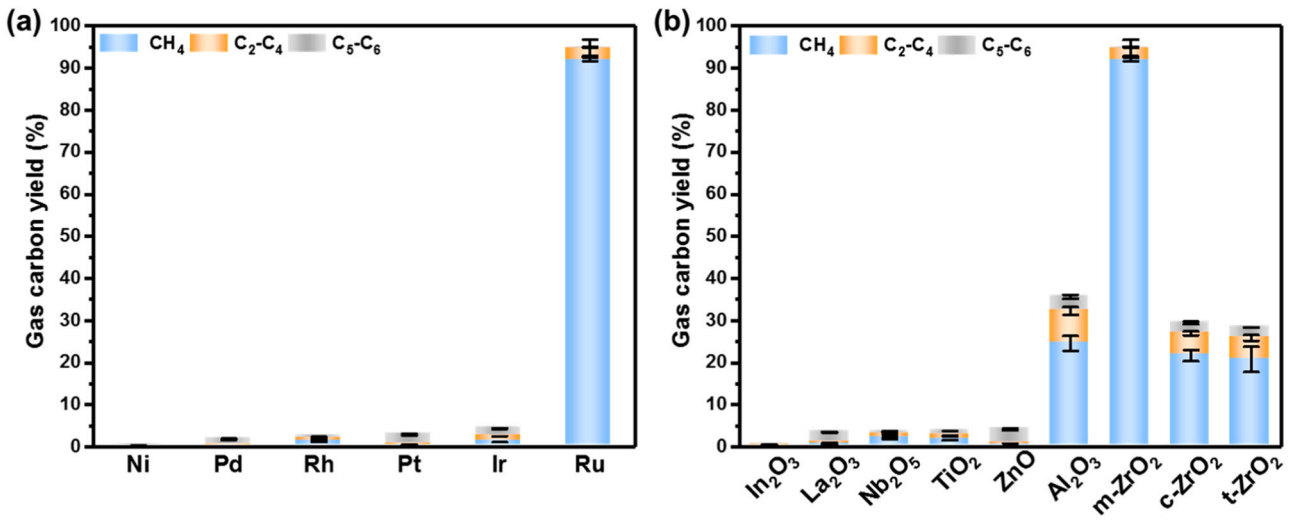

Fig. 1. (a) Effect of different metal catalysts supported on m-ZrO_2 for the conversion of natural rubber. Reaction condition: natural rubber (0.5 g), catalysts (0.1 g), 290 °C, 3 MPa H_2, 2 h. (b) Effect of different supports for the conversion of natural rubber over Ru-based catalyst. Reaction condition: natural rubber (0.5 g), catalyst (0.1 g), 290 °C, 3 MPa H_2, 2 h.

would limit the further separation and cleavage of C-C bonds to gas products. Although we have studied the catalytic hydrogenolysis of C-O and C-C bonds in raw biomass to efficiently produce natural gas over Ni and Ru-based catalysts [27,28], the catalytic complete cleavage of the inert C═C and C-C bonds in natural rubber under mild reaction conditions still remains challenging.

Considering the crucial role of supports in the heterogeneous catalysts, the metal-support synergistic effect could greatly enhance the catalytic activity by a subtle catalyst design [29–31]. For the catalytic hydrogenation, it occurred the hydrogen dissociation on metal Pt and Ru [32,33], while the acid sites of supports normally acted as the activated adsorption and hydrogenation site. Thus, the regulation of acid sites would have a significant impact on the catalytic performance by the synergistic effect. ZrO_2, a typical reducible support with the controlled acid sites, has been widely applied for the hydrogenation and cracking reactions [34,35]. Especially, ZrO_2 with different crystal type greatly influenced the catalytic hydrogenolysis reaction by the oxygen vacancy, electron distribution, acid-base sites and so on [36–38]. Therefore, it shed the lights to ZrO_2 supported metal catalyst design for the efficient hydrogenolysis of natural rubber wastes to achieve high yield gas products.

In this study, we reported an efficient approach to catalyze complete cleavage of the inert chemical bonds in natural rubber wastes. The catalytic activity of Ru-based catalysts was enhanced by the crystal phase regulation of ZrO_2 support. Ru/m-ZrO_2 could catalyze conversion of natural rubber to acquire 95.0% of gas carbon yield, which was comprised of 98.6 mol% of CH_4 and only 1.4 mol% of C2-C4 hydrocarbons and similar in composition of commercial natural gas. The study of reaction pathway showed that the natural rubber underwent the hydrogenation of C═C bonds and further hydrogenolysis of C-C bonds. The Ru^0 species and spill-over hydrogen in Ru/m-ZrO_2 had the synergistic effect on the catalytic conversion of natural rubber to natural gas.

2. Experimental section

2.1. Preparation of catalysts

Ru/m-ZrO_2 was synthesized by initial wet impregnation. $RuCl_3{\cdot}xH_2O$ was dissolved into Milli-Q water as a precursor. Then the precursor was impregnated with the m-ZrO_2 support under stirring. The mixture was further treated by ultrasound. The beaker was sealed, the metal precursor and supports were impregnated at ambient temperature, and then the solvent was evaporated in a 110 °C oven. The impregnated catalyst was reduced at 250 °C for 3 h in a tubular furnace in the hydrogen atmosphere. After the tubular furnace was cooled down, the flow gas in the tube was switched to nitrogen. When using the catalyst, it was transferred from the tubular furnace to the reactor immediately. Ru/c-ZrO_2, Ru/t-ZrO_2, Ru/Al_2O_3, Ru/ZnO, Ru/TiO_2, Ru/Nb_2O_5, Ru/La_2O_3, Ru/In_2O_3 and different metals (Ir, Rh, Pt, Pd and Ni) supported on m-ZrO_2 catalysts were obtained by the same procedure. Exceptionally, m-ZrO_2 supported Ni was reduced at 450 °C for 3 h.

2.2. Catalytic conversion of natural rubber

The catalytic conversion of natural rubber and rubber wastes were operated in a 50 mL Parr autoclave. Reactants include natural rubber, balloon, stopper, ear washing bulb, tube, pillow and squalene. Firstly, the reactants (0.1–0.5 g) were loaded into the reactor, followed by the catalyst (0.1 g) which was added rapidly. Then the reactor was sealed, N_2 was exchanged for 3 times to discharge the air, and then H_2 was exchanged for 5 times to discharge the N_2, 0.1–4 MPa H_2 was filled. The reactants were mixed and rapidly heated to the designed temperature (270–300 °C) under stirring of 700 rpm. After the designated reaction time (10–300 min), the reactor was firstly cooled to about 150 °C in air. Then the reactor was placed in an ice-water bath to further cool to the ambient temperature. The temperature and pressure were monitored and recorded after the reaction for subsequent analysis. Then, the gas after reaction was collected with a gas collection bag for further analysis. After the gas in the reactor was exhausted, the reactor was opened and 5 mL dichloromethane was added, and the suspension was collected and filtered for further analysis.

2.3. Analysis of gas and liquid products

According to our previous analytical method for the production of natural gas [27,28,39], the gas products from the hydrogenolysis of natural rubber and rubber wastes were analyzed by gas chromatographs (Agilent 7890 A and Agilent 7890B GC). The chromatographic column, detector and detailed method parameters of gas chromatograph was consistent with those in our previous methods. The standard gas mixtures involving normal alkanes (C1-C6), hydrogen, carbon dioxide, nitrogen, helium, and argon were used for quantitative calculations of gas products. Based on reactor volume and these peak area ratios detected by GC, the content of each component was further determined combined

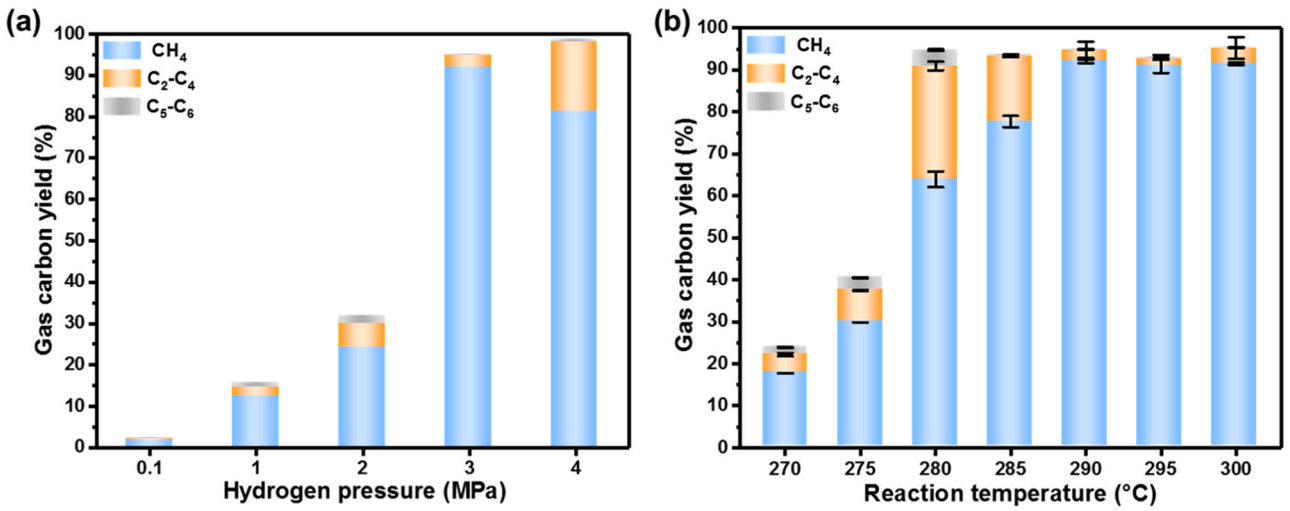

Fig. 2. (a) Effect of initial hydrogen pressure on the catalytic conversion of natural rubber. Reaction condition: natural rubber (0.5 g), Ru/m-ZrO_2 (0.1 g), 290 °C, 2 h. (b) Effect of operated temperature on the catalytic conversion of natural rubber. Reaction condition: natural rubber (0.5 g), Ru/m-ZrO_2 (0.1 g), 3 MPa H_2, 2 h.

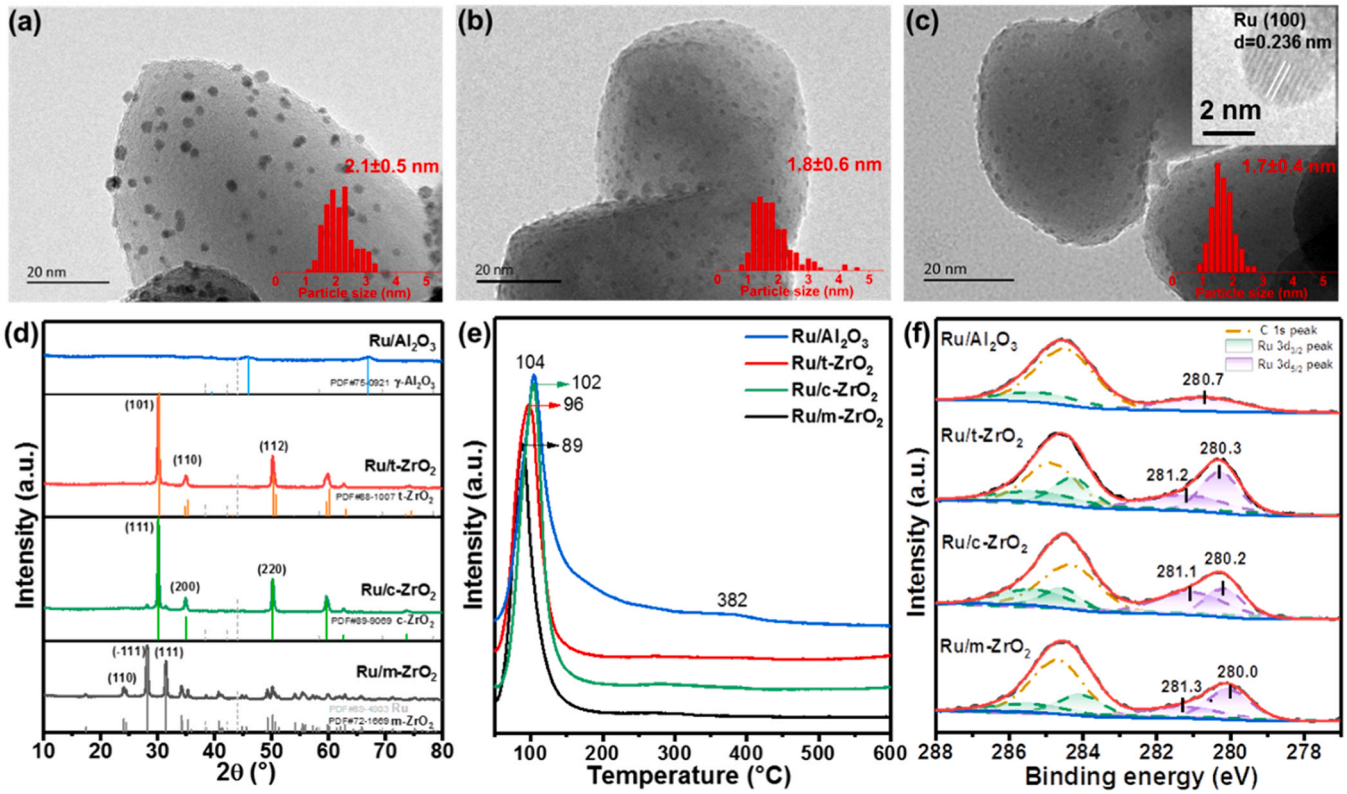

Fig. 3. TEM images and the corresponding size distributions of Ru nanoparticles from (a) Ru/t-ZrO_2. (b) Ru/c-ZrO_2. (c) Ru/m-ZrO_2. (d) XRD analysis of Ru-based catalysts. (e) H_2-TPR profiles of Ru-based catalysts. (f) XPS spectrum of Ru 3d region for the different Ru-based catalysts.

with the temperature and pressure after the reaction by the Ideal Gas Equation.

The gas carbon yield was determined by the following equation:

$$\text{Gas carbon yield}\ (\%) = \frac{n_{CH4} + n_{CO2} + 2n_{C2H6} + 3n_{C3H8} + 4n_{C4H10} + 5n_{C5H12} + 6n_{C6H14}}{\text{reactants weight} \times \text{the percentage of carbon in reactants} \div 12} \times 100\% \quad (1)$$

where, n was the mole numbers of different gas products.

The mole percentage of different gas in products distribution was determined by the following equation:

$$Molar\ percentage\ of\ each\ gas\ in\ products\ distribution\ (mol\%) = \frac{mole\ nomber\ of\ each\ gas}{total\ mole\ number\ of\ gas\ products} \times 100\% \quad (2)$$

The liquid phase products after the catalytic hydrogenolysis of natural rubber and squalene were detected by GC, and further detected by comprehensive two-dimensional GC coupled to time-of-flight mass spectrometry (GC×GC-TOFMS) and GC-mass spectrometry (GC-MS).

3. Results and discussion

3.1. Catalytic conversion of natural rubber

The used catalysts in this study were synthesized according to the incipient wetness impregnation method, which were applied for the catalytic transformation of natural rubber. As the metal species had a great influence on the catalytic performance, the different metal catalysts were firstly investigated for the natural rubber hydrogenolysis. As shown in Fig. 1a, almost no gas products were detected over the non-noble metal catalyst of Ni/m-ZrO_2. The noble metal catalysts mainly involved Pd, Rh, Pt and Ir supported on m-ZrO_2, and the generated gas carbon yield stayed below 5% from the conversion of natural rubber (Table S1). In contrast, Ru/m-ZrO_2 afforded 95.0% of gas carbon yield under the same operating conditions, demonstrating that Ru species revealed the high catalytic activity for the natural rubber hydrogenolysis.

In view of the impact of supports on the catalytic performance, Ru supported on different oxides was further investigated for the catalytic hydrogenolysis of natural rubber. Fig. 1b showed that Ru supported on In_2O_3, La_2O_3, Nb_2O_5, TiO_2 and ZnO displayed the low catalytic activity for the conversion of natural rubber with the gas carbon yield less than 5%. When Ru/Al_2O_3 was used, the high gas carbon yield of 35.7% was obtained (Table S2). However, Ru/m-ZrO_2 achieved 95.0% of gas carbon yield from the natural rubber hydrogenolysis, which was more than 2 times higher than that of Ru/Al_2O_3. Furthermore, ZrO_2 support with different crystal phases was also studied, Ru/c-ZrO_2 and Ru/t-ZrO_2 gave 29.5 and 28.3% of gas carbon yield, which was much lower than that of Ru/m-ZrO_2. Thus, Ru supported on m-ZrO_2 displayed the best catalytic performance for the transformation of natural rubber into gas products.

As the initial hydrogen pressure would greatly affect the generated gas products, the influence of hydrogen pressure on the conversion of natural rubber was studied. As illustrated in Fig. 2a, when the initial hydrogen pressure increased from 0.1 to 3 MPa, the gas carbon yield gradually varied from 2.0% to 95.0%. With the initial hydrogen pressure further increasing to 4 MPa, the gas carbon yield slightly increased to 98.7%. Whereas, the molar percentage of CH_4 sharply decreased from 98.6 to 91.4 mol% with the simultaneously increased molar percentage of C2-C6 alkanes in gas products (Table S3). The reaction results indicated that the higher initial hydrogen pressure would inhibit the further catalytic hydrogenolysis reaction. The influence of reaction temperature on gas carbon yield and detailed gas products distribution was illustrated in Fig. 2b. When the reaction temperature increased from 270 to 280 °C, the gas carbon yield increased to 94.7%, and the molar percentage of CH_4 and C2-C4 alkanes in gas products were 85.9 and 13.1 mol%, respectively (Table S4). As the reaction temperature further increased to 290 °C, the gas carbon yield for the catalytic transformation of natural rubber remained almost unchanged, while the molar percentage of CH_4 increased to 98.6% with C2-C4 alkanes molar percentage concurrently decreased to 1.4 mol%. Ultimately, the gas carbon yield and detailed products percentage were nearly unchanged, which was similar to the composition of commercial natural gas. The above results indicated that Ru supported on m-ZrO_2 exhibited the excellent catalytic activity for the direct conversion of natural rubber to natural gas.

3.2. Characterization of the catalysts

The nitrogen sorption isotherm of ZrO_2 with different crystal phases exhibited a typical IV isotherm with a H3 typed hysteresis, suggesting the mesopores characteristics (Fig. S1) [40]. The Brunauer-Emmett-Teller (BET) surface area and total pore volume of ZrO_2 supports were approximate, which was measured to be 21.4 m^2/g and 0.138 cm^3/g for m-ZrO_2 (Table S5) and much smaller than that of Al_2O_3. The transmission electron microscopy (TEM) was carried out to study the morphology of Ru-based catalysts with the detailed Ru nanoparticles size distribution. Fig. 3a showed that the mean size of Ru nanoparticles supported on t-ZrO_2 was 2.1 nm. When Al_2O_3 and c-ZrO_2 were used as supports, the mean size of Ru was both 1.8 nm with some nanoparticles size more than 3.0 nm (Fig. 3b and S2). Further for m-ZrO_2, the different crystal planes were observed for ZrO_2 supports with the different crystal phases (Fig. S3). And m-ZrO_2 supported Ru nanoparticle size ranged from 0.8 to 2.8 nm with the mean diameter slightly decreasing to 1.7 nm, which was evenly dispersed without the obviously formed aggregations (Fig. 3c). Additionally, the lattice fringe of 0.236 nm in Ru/m-ZrO_2 was assigned to Ru(100) plane.

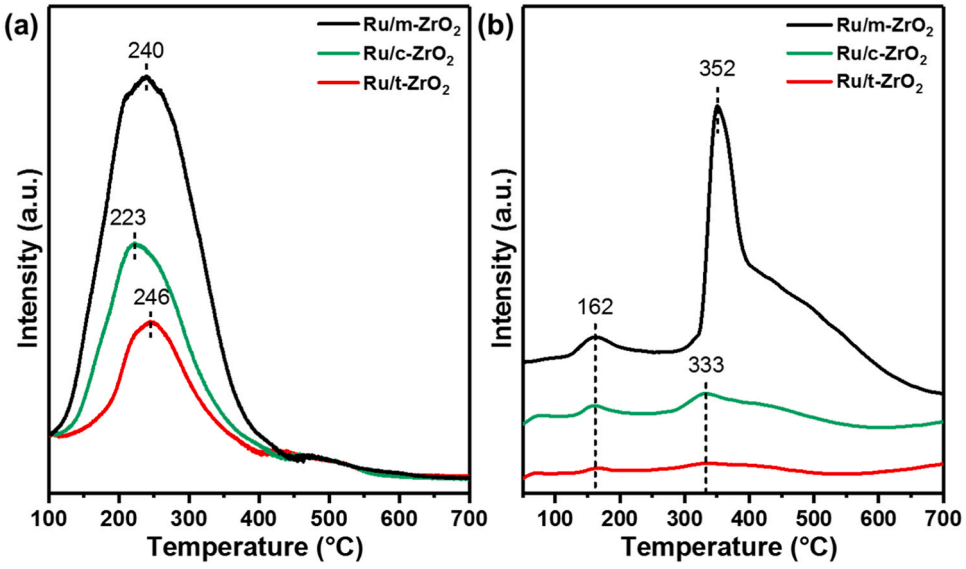

Fig. 4. (a) NH_3-TPD and (b) H_2-TPD profiles of the prepared Ru-based catalysts supported on ZrO_2.

X-ray powder diffraction (XRD) patterns of the prepared Ru-based catalysts were conducted and displayed in Fig. 3d. These catalysts mainly revealed the characteristic peaks of the corresponding supports, such as γ-Al_2O_3 (PDF#75–0921). The t-ZrO_2 revealed the main diffraction peaks at 2θ = 30.3, 34.8, 35.2, 50.4, 50.7, 59.6 and 60.2°, c-ZrO_2 displayed the diffraction peaks at 2θ = 30.1, 34.9, 50.2, 59.7 and 81.7°, while the characteristic peaks of m-ZrO_2 was at 24.0, 24.5, 28.2, 31.5, 34.2, 34.4, 35.3, 40.7, 49.3, 50.1 and 50.6°, indicating the tetragonal (PDF#88–1007), cubic (PDF#89–9069) and monoclinic (PDF#72–1669) of ZrO_2 supports [41–43]. And the crystal phases were maintained after the impregnation and reduction treatment of Ru-based catalysts. Moreover, no obvious diffraction peaks of Ru metal were observed, which indicated that Ru particles were well dispersed in these supports. The above results were in accordance with TEM analysis.

The reducibility of different Ru-based catalysts was studied by H_2 temperature programmed reduction (H_2-TPR) measurement. Since the supports were stable and hard to be reduced [44], a main peak appeared at around 100 °C in the H_2-TPR profile was ascribed to the reduction of supported Ru species to Ru metal (Fig. 3e) [45,46]. While for Ru/Al_2O_3, a weak reduction peak at 382 °C was observed, which might be caused by the metal-support interaction of Ru species and Al_2O_3 support [47]. For the supported Ru on the different crystal phases of ZrO_2, the reduction temperature of Ru/m-ZrO_2 was 89 °C, which was slightly lower than that of Ru/t-ZrO_2 and Ru/c-ZrO_2 catalysts. This low reduction temperature might be attributed to the well-dispersed Ru on m-ZrO_2 support with the small average diameter, which was easier to be reduced.

X-ray photoelectron spectroscopy (XPS) was conducted to study the chemical state of the supported Ru-based catalysts, the corresponding Ru 3d core level spectrum was shown in Fig. 3f. After the reduction of Ru-based catalysts at 250 °C, Al_2O_3 and In_2O_3 supported Ru displayed a Ru $3d_{5/2}$ peak at 280.7 and 280.4 eV (Fig. S4), corresponding to ruthenium with the positive charge, which demonstrated the existence of $Ru^{\delta+}$ species. In comparison with Ru/Al_2O_3, Ru supported on ZrO_2 with the different crystal phases further revealed another peak with the low binding energy (BE) values of Ru $3d_{5/2}$, suggesting that ZrO_2 supported Ru species were relatively easy to be reduced, which fitted with the above H_2-TPR results. Moreover, Ru/m-ZrO_2 displayed the lower BE values than and Ru/t-ZrO_2 and Ru/c-ZrO_2, which was at 280.0 eV and assigned to Ru^0 [45,48]. Eventually, most of Ru species in Ru/m-ZrO_2 were reduced to metallic Ru.

Moreover, in-situ diffuse reflectance infrared Fourier transform (DRIFT) spectra of CO adsorption was also used to analyze the electronic states of supported metals based on the CO adsorption on metal sites [49,50]. The CO absorption band of 1990–2060 and 2060–2156 cm^{-1} were attributed to the CO adsorption on the Ru^0 and $Ru^{\delta+}$ species, respectively. For Ru/m-ZrO_2, the intensity of the CO adsorption peaks for the Ru^0 species at 1959 and 2029 cm^{-1} were significantly higher than that for the $Ru^{\delta+}$ species at 2072 and 2130 cm^{-1} (Fig. S5). Whereas, for Ru/c-ZrO_2 catalyst, the intensity of the CO adsorption peaks for the Ru^0 species was lower than that for the $Ru^{\delta+}$ species. These results indicated that the proportion of the Ru^0 species in Ru/m-ZrO_2 is higher than that of the $Ru^{\delta+}$ species, which was opposite for Ru/c-ZrO_2.

The surface acidic and basic properties of the prepared Ru-based catalysts were measured by the temperature programmed desorption of NH_3 and CO_2 (NH_3- and CO_2-TPD), as illustrated in Fig. 4a and S6. The prepared Ru-based displayed the higher acidity than basicity (Table S6). Fig. S6 showed the weak, medium and strong base sites in CO_2 desorption profiles [45,51]. And the base sites concentration was approximate for ZrO_2 supported Ru-based catalysts. In NH_3-TPD profiles, Fig. 4a mainly revealed one broad peak at approximately 240 °C, which was related to medium acid sites [52]. The weak peak located at about 450 °C corresponded to strong acid sites. Ru/Al_2O_3 catalyst exhibited the highest amount of acid sites (Fig. S7 and Table S6). While for the different crystal phases of ZrO_2 supported Ru-based catalysts, the amounts of acid sites were greatly different, which was higher for

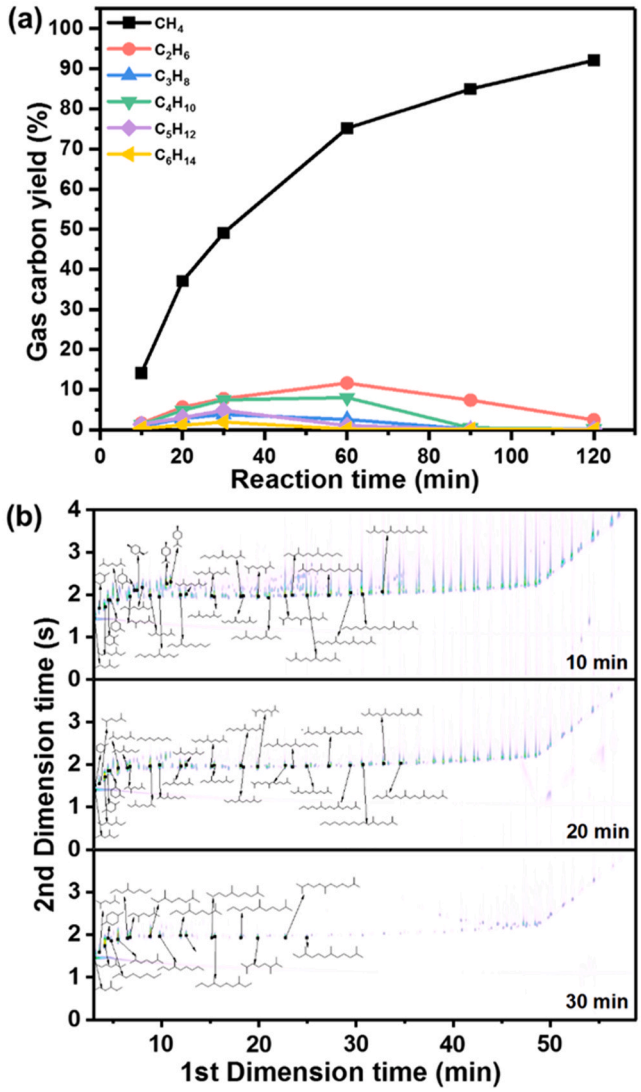

Fig. 5. (a) The gas carbon yield from the natural rubber hydrogenolysis with different reaction times. (b) GC×GC-TOFMS analysis of liquid products from the natural rubber hydrogenolysis with different reaction times. Reaction condition: natural rubber (0.5 g), Ru/m-ZrO_2 (0.1 g), 290 °C, 3 MPa H_2.

Ru/m-ZrO_2 (69.66 μmol NH_3/g cat). Thus, the acidity of Ru/ZrO_2 catalyst was enhanced with the monoclinic crystal phase of ZrO_2 support.

The H_2 temperature programmed desorption (H_2-TPD) profiles of ZrO_2 supported Ru-based catalysts were conducted to evaluate the interaction of catalysts and hydrogen during this reaction. As presented in Fig. 4b and S8, the minor peak at below 300 °C was usually assigned to the physics hydrogen desorption from Ru components. Ru/m-ZrO_2 appeared the slightly increased intensity compared with Ru/c-ZrO_2 and Ru/t-ZrO_2, and Ru/Al_2O_3 showed the peak with high intensity, indicating the more weakly chemisorbed and thus reactively chemisorbed hydrogen [53]. Another hydrogen desorption peak at the high temperature (>300 °C) could be attributed to the existed hydrogen spillover from Ru sites to support [52]. The high intensity of peak at around 378 °C suggested the existed hydrogen spillover in Ru/Al_2O_3. Most importantly, the hydrogen desorption peak intensity of Ru/m-ZrO_2 was much stronger than that of Ru/c-ZrO_2 and Ru/t-ZrO_2, and the increased acid sites in prepared Ru-based catalysts enhanced the spillover of hydrogen [48]. Therefore, compared to Ru/c-ZrO_2 and Ru/t-ZrO_2, Ru/m-ZrO_2 displayed the significant ability to promote the hydrogen spillover and anchor the spill-over hydrogen.

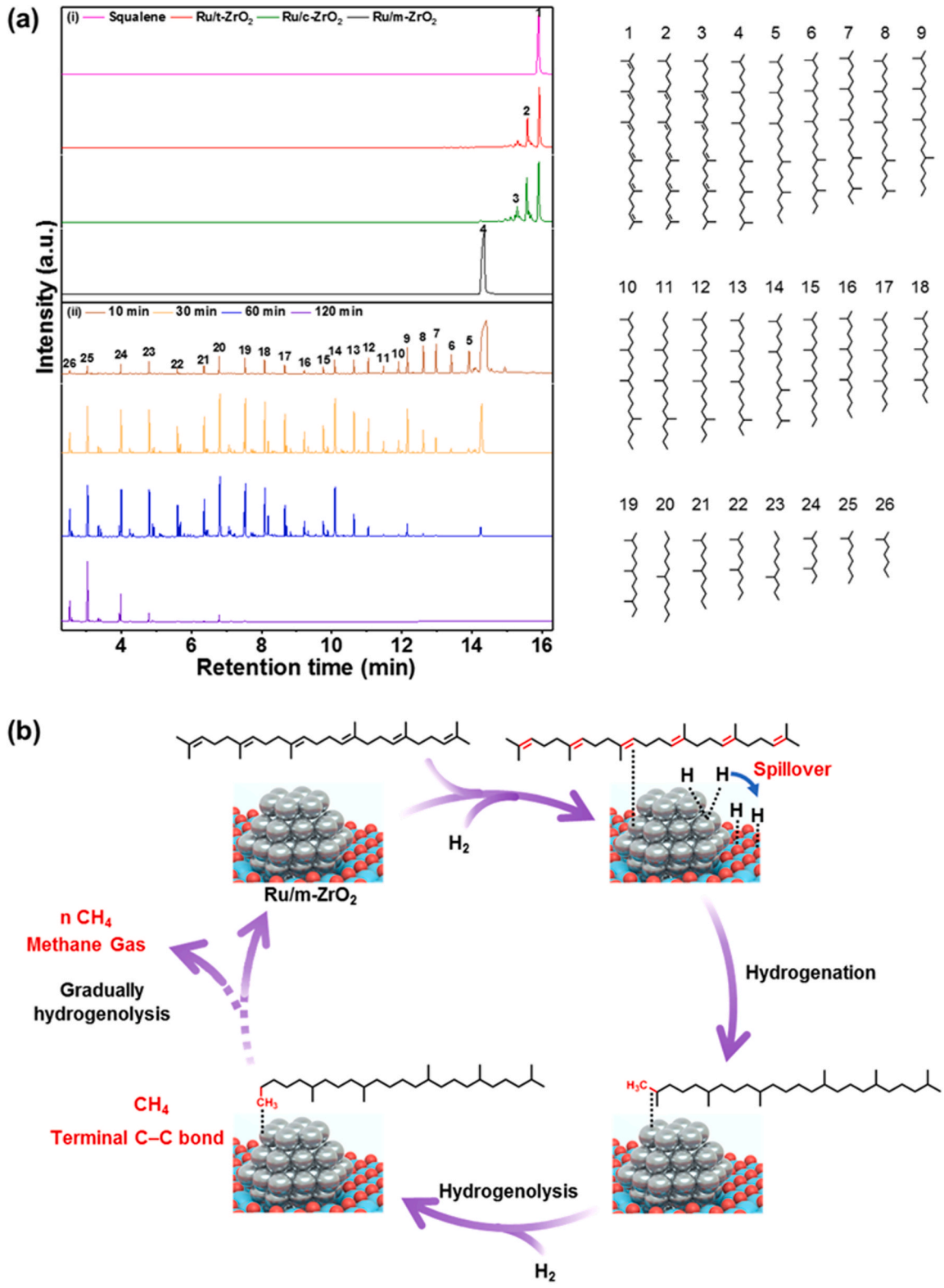

Fig. 6. (a) GC-MS analysis of liquid products from the squalene conversion with different Ru-based catalysts or reaction times. Reaction condition: (i) squalene (0.5 g), Ru-based catalysts (0.03 g), 60 °C, 3 MPa H_2, 10 min, (ii) squalene (0.5 g), Ru/m-ZrO_2 (0.1 g), 230 °C, 3 MPa H_2. (b) The reaction pathway of C═C bonds hydrogenation and C-C bonds hydrogenolysis in squalene over Ru/m-ZrO_2.

3.3. Reaction pathway for the catalytic hydrogenolysis of natural rubber

To investigate the reaction pathway for catalytic hydrogenolysis of natural rubber, the influence of reaction time on gas and liquid carbon products was studied (Fig. 5). As the reaction time prolonged from 10 to 120 min, the CH_4 gas carbon yield rapidly increased from 14.2% to 92.1% (Fig. 5a and Table S7). Whereas, the carbon yield of C2-C6 alkanes firstly increased with the extended reaction time, and then

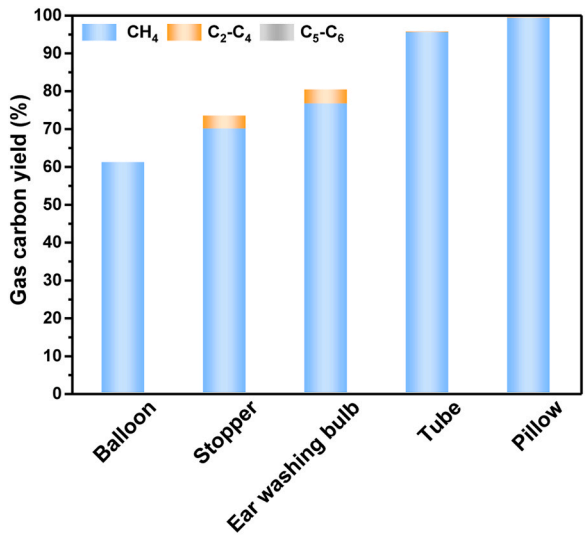

Fig. 7. Catalytic conversion of rubber wastes over Ru/m-ZrO_2 catalyst. Reaction condition: reactants (0.1 g), Ru/m-ZrO_2 (0.2 g), 290 °C, 3 MPa H_2, 5 h.

decreased for the further catalytic hydrogenolysis. The remaining liquid products were analyzed with GC×GC-TOF MS and GC-MS. GC×GC-TOF MS results showed that the carbon chain length and the signal intensity gradually decreased with increasing the reaction time, which was consistent with GC-MS analysis (Fig. 5b and S9). In addition, the detailed structure analysis for the liquid products was saturated alkanes and no alkenes were detected, indicating that the first hydrogenation of C═C bonds in natural rubber occurred over Ru/m-ZrO_2. Thus, the catalytic transformation of natural rubber would undergo the hydrogenation of C═C bonds and further hydrogenolysis of C-C bonds to acquire natural gas.

Due to the complex structure of liquid products from the catalytic natural rubber hydrogenolysis, squalene with six isoprene units was chosen as the simple model compound to further investigate the reaction pathway of C═C bonds hydrogenation and C-C bonds hydrogenolysis over Ru/m-ZrO_2. As shown in Fig. 6a, GC-MS analysis displayed a peak for squalene with the retention time at 15.7 min. After the catalytic conversion over Ru-based catalysts with the different crystal phases of ZrO_2, a small amount of squalene was converted to the partial hydrogenation products of compounds **2** and **3** over Ru/t-ZrO_2 and Ru/c-ZrO_2. In contrast, it only detected the complete hydrogenation product of squalane over Ru/m-ZrO_2 under the same reaction conditions. Thus, the spill-over hydrogen on Ru/m-ZrO_2 facilitated the hydrogenation of squalene to squalane. For the further catalytic hydrogenolysis with the different reaction time, it showed the liquid products of saturated alkanes with one main peak for squalane at 10 min, and the low gas carbon yield of 5.2% was obtained (Table S8). Further for the increased reaction time, the carbon chain length of liquid products gradually reduced with the increased gas carbon yield. Therefore, the gas products came from the gradual hydrogenolysis of C-C bonds in the squalane main chain (Fig. 6b). As the bond energy of C═C bonds was about 2 times higher than that of C-C bonds, the primary hydrogenation of C═C bonds would promote the hydrogenolysis of squalene to achieve the high yield of natural gas.

For the catalytic hydrogenolysis of natural rubber to natural gas, the metal sites and spill-over hydrogen played a vital role in the catalytic hydrogenation of C═C bonds and hydrogenolysis of C-C bonds. Compared with c-ZrO_2 and t-ZrO_2, m-ZrO_2 with more acid sites facilitated the hydrogen spillover and further anchored the spill-over hydrogen in Ru/m-ZrO_2, which could make the great contribution to the catalytic hydrogenation of C═C bonds. For the subsequent catalytic hydrogenolysis of C-C bonds to gas products, although Al_2O_3 possessed the high acid sites and spill-over hydrogen, the existed $Ru^{\delta+}$ species in Ru/Al_2O_3 would affect the hydrogenolysis of C-C bonds. Furthermore, for the ZrO_2 support with different crystal phases, m-ZrO_2 supported Ru catalyst were highly dispersed and easy to be reduced. The Ru^0 species in Ru/m-ZrO_2 catalyst revealed the high catalytic performance for the hydrogenolysis of C-C bonds to directly acquire 95.0% of natural gas carbon yield, which was much higher than the gas carbon yield over Ru/c-ZrO_2 and Ru/t-ZrO_2 catalysts. Overall, the Ru^0 species and spill-over hydrogen in Ru/m-ZrO_2 catalyst had the synergistic effect on the catalytic transformation of natural rubber to natural gas, which displayed the outstanding reaction activity during the catalytic hydrogenation of C═C bonds and hydrogenolysis of C-C bonds.

3.4. Catalytic conversion of natural rubber wastes

The natural rubber wastes including balloon, stopper, ear washing bulb, tube and pillow were further applied for the catalytic hydrogenolysis to natural gas. As shown in Fig. 7, balloon and stopper wastes gave 61.1 and 73.5% of gas carbon yield, with the CH_4 molar percentage more than 97 mol%. The gas carbon yield of 80.4% was obtained when ear washing bulb was converted over Ru/m-ZrO_2 (Table S9 and S10). Ultimately, for the tube and pillow catalytic conversion from natural rubber wastes, it achieved 95.8 and 99.6% of gas carbon yield accompanied with the CH_4 molar percentage of 99.9 mol%. Thus, the various natural rubber wastes were directly transformed into natural gas in our developed process.

According to the above results, a concise Sankey diagram was depicted for the catalytic transformation of natural rubber combined with hydrogen into natural gas, which was based on the mass balance (Fig. 8). It revealed that 95.0% of organic carbon in natural rubber was converted to gas products with the CH_4 and C2-C6 alkanes carbon yield of 92.1 and 2.9%, respectively. The others included a small amount of deposited carbon species (Fig. S10). On the basis of this results, 1 kg of natural rubber was predicted to produce 1612 L natural gas, which was constituted by 98.6% of CH_4 and 1.4% of C2-C6 alkanes.

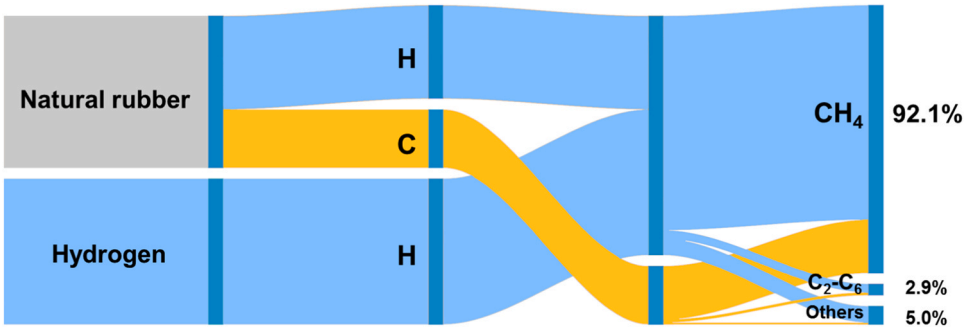

Fig. 8. Sankey diagram for the catalytic transformation of natural rubber into natural gas based on the mass balance. Reaction condition: natural rubber (0.5 g), Ru/m-ZrO_2 (0.1 g), 3 MPa H_2, 290 °C, 2 h.

4. Conclusions

Overall, an efficient approach for the directly transformation of natural rubber to natural gas with high atom economy was developed under the mild condition. This process achieved the complete cleavage of the inert chemical bonds in natural rubber by the enhanced catalytic activity of Ru/ZrO_2 with the modulated support crystal phases. The generated gas carbon yield was up to 95.0% accompanied with 98.6 mol % of CH_4 and only 1.4 mol% of C2-C4 alkanes, which was similar to commercial natural gas composition. The reaction pathway showed that the natural rubber firstly underwent the hydrogenation of C═C bonds, which was promoted by the hydrogen spillover in $Ru/m\text{-}ZrO_2$. Meanwhile, the Ru^0 species in $Ru/m\text{-}ZrO_2$ revealed the high catalytic activity for the gradual hydrogenolysis of C-C bonds in the rubber main chain. Eventually, different rubber wastes involving rubber stopper and tube were also directly converted to natural gas, facilitating the carbon-neutral development in the future.

CRediT authorship contribution statement

Xiaoqin Si: Writing – review & editing, Methodology, Funding acquisition. **Zhiwen Ren:** Writing – original draft, Investigation, Data curation. **Mengjie Li:** Validation. **Qian Liu:** Investigation. **Rui Lu:** Validation. **Hao Chen:** Validation. **Fang Lu:** Writing – review & editing, Supervision, Funding acquisition, Conceptualization. **Hongliang Liang:** Software.

Declaration of Competing Interest

The authors declare that they have no known competing financial interests or personal relationships that could have appeared to influence the work reported in this paper.

Data Availability

Data will be made available on request.

Acknowledgments

This work was supported by National Natural Science Foundation of China (22208339), National Key R&D Program of China (2019YFC1905303) and Youth Innovation Fund of Dalian Institute of Chemical Physics (DICP I202132).

Appendix A. Supporting information

Supplementary data associated with this article can be found in the online version at doi:10.1016/j.apcatb.2024.123988.

References

[1] L.R.G. Treloar, Rubbers and their characteristics: real and ideal, Nature 155 (1945) 441–444.
[2] H.J. Wing, Carbon and hydrogen in rubber hydrocarbon, Science 105 (1947) 363–364.
[3] H.M. Nor, J.R. Ebdon, Telechelic liquid natural rubber: a review, Prog. Polym. Sci. 23 (1998) 143–177.
[4] J.M.M. Martinez, Natural rubber by a rubber man, Mater. Today 9 (2006) 55.
[5] L. Asaro, M. Gratton, N. Poirot, S. Seghar, N. Aït Hocine, Devulcanization of natural rubber industry waste in supercritical carbon dioxide combined with diphenyl disulfide, Waste Manag. 118 (2020) 647–654.
[6] H. Mark, Natural and artificial rubber: the elasticity of long-chain molecules, Nature 141 (1938) 670–672.
[7] B.S. Gaut, Natural rubber and the Russian dandelion genome, Natl. Sci. Rev. 5 (2018) 88–89.
[8] G.E. Coombs, The uses of rubber, Nature 135 (1935) 417–418.
[9] K. Lee, Y. Jing, Y. Wang, N. Yan, A unified view on catalytic conversion of biomass and waste plastics, Nat. Rev. Chem. 6 (2022) 635–652.
[10] H. Chen, K. Wan, Y. Zhang, Y. Wang, Waste to wealth: Chemical recycling and chemical upcycling of waste plastics for a great future, ChemSusChem 14 (2021) 4123–4136.
[11] G.S. Miguel, J. Aguado, D.P. Serrano, J.M. Escola, Thermal and catalytic conversion of used tyre rubber and its polymeric constituents using Py-GC/MS, Appl. Catal. B: Environ. 64 (2006) 209–219.
[12] C. Roy, H. Darmstadt, B. Benallal, C. Amen-Chen, Characterization of naphtha and carbon black obtained by vacuum pyrolysis of polyisoprene rubber, Fuel Process. Technol. 50 (1997) 87–103.
[13] S. Ramarad, M. Khalid, C.T. Ratnam, A.L. Chuah, W. Rashmi, Waste tire rubber in polymer blends: A review on the evolution, properties and future, Prog. Mater. Sci. 72 (2015) 100–140.
[14] S. Singh, W. Nimmo, M.T. Javed, P.T. Williams, Cocombustion of pulverized coal with waste plastic and tire rubber powders, Energy Fuels 25 (2011) 108–118.
[15] L. Zhang, B. Zhou, P. Duan, F. Wang, Y. Xu, Hydrothermal conversion of scrap tire to liquid fuel, Chem. Eng. J. 285 (2016) 157–163.
[16] F. Sadaka, I. Campistron, A. Laguerre, J.F. Pilard, Controlled chemical degradation of natural rubber using periodic acid: Application for recycling waste tyre rubber, Polym. Degrad. Stab. 97 (2012) 816–828.
[17] K.P. Sullivan, A.Z. Werner, K.J. Ramirez, L.D. Ellis, J.R. Bussard, B.A. Black, D. G. Brandner, F. Bratti, B.L. Buss, X. Dong, S.J. Haugen, M.A. Ingraham, M. O. Konev, W.E. Michener, J. Miscall, I. Pardo, S.P. Woodworth, A.M. Guss, Y. Román-Leshkov, S.S. Stahl, G.T. Beckham, Mixed plastics waste valorization through tandem chemical oxidation and biological funneling, Science 378 (2022) 207–211.
[18] J.D. Martínez, N. Puy, R. Murillo, T. García, M.V. Navarro, A.M. Mastral, Waste tyre pyrolysis – a review, Renew. Sustain. Energy Rev. 23 (2013) 179–213.
[19] I. Ahmed, A.K. Gupta, Characteristic of hydrogen and syngas evolution from gasification and pyrolysis of rubber, Int. J. Hydrog. Energy 36 (2011) 4340–4347.
[20] N.H. Zerin, M.G. Rasul, M.I. Jahirul, A.S.M. Sayem, End-of-life tyre conversion to energy: A review on pyrolysis and activated carbon production processes and their challenges, Sci. Total Environ. 905 (2023) 166981.
[21] C. Yang, R. Fu, Q. Jiao, J. Yu, J. Liang, H. Zhu, X. Jiao, C. Feng, Y. Zhang, H. Li, Y. Zhao, Catalytic cracking of waste tires using nano-ZSM-5/MgAl-LDO, Energy Technol. 10 (2022) 2200186.
[22] Z. Li, L. Tao, Q. Yang, L. Chen, H. Qi, X. Ma, H. Ben, Mechanism research on hydrogen production from catalytic pyrolysis of waste tire rubber, Fuel 331 (2023) 125846.
[23] A. Hijazi, A.H. Al-Muhtaseb, S. Aouad, M.N. Ahmad, J. Zeaiter, Pyrolysis of waste rubber tires with palladium doped zeolite, J. Environ. Chem. Eng. 7 (2019) 103451.
[24] A. Mahittikul, P. Prasassarakich, G.L. Rempel, Hydrogenation of natural rubber latex in the presence of $[Ir(cod)(PCy_3)(py)]PF_6$, J. Mol. Catal. A: Chem. 297 (2009) 135–141.
[25] S. Bhattacharjee, A.K. Bhowmick, B.N. Avasthi, Hydrogenation of epoxidized natural rubber in the presence of palladium acetate catalyst, Polymer 34 (1993) 5168–5173.
[26] T. Tan, W. Wang, K. Zhang, Z. Zhan, W. Deng, Q. Zhang, Y. Wang, Upcycling plastic wastes into value-added products by heterogeneous catalysis, ChemSusChem 15 (2022) e202200522.
[27] X. Si, R. Lu, Z. Zhao, X. Yang, F. Wang, H. Jiang, X. Luo, A. Wang, Z. Feng, J. Xu, F. Lu, Catalytic production of low-carbon footprint sustainable natural gas, Nat. Commun. 13 (2022) 258.
[28] Z. Ren, X. Si, J. Chen, X. Li, F. Lu, Catalytic complete cleavage of C-O and C-C bonds in biomass to natural gas over Ru(0), ACS Catal. 12 (2022) 5549–5558.
[29] W. Gao, Y. Zhao, H. Chen, H. Chen, Y. Li, S. He, Y. Zhang, M. Wei, D.G. Evans, X. Duan, Core-shell $Cu@(CuCo\text{-}alloy)/Al_2O_3$ catalysts for the synthesis of higher alcohols from syngas, Green. Chem. 17 (2015) 1525–1534.
[30] M.M. Hossain, K.E. Sedor, H.I. de Lasa, $Co\text{-}Ni/Al_2O_3$ oxygen supports for fluidized bed chemical-looping combustion: Desorption kinetics and metal-support interaction, Chem. Eng. Sci. 62 (2007) 5464–5472.
[31] H. Jiang, T. Akita, T. Ishida, M. Haruta, Q. Xu, Synergistic catalysis of Au@Ag core-shell nanoparticles stabilized on metal-organic framework, J. Am. Chem. Soc. 133 (2011) 1304–1306.
[32] M.Y. Byun, Y.E. Kim, J.H. Baek, J. Jae, M.S. Lee, Effect of surface properties of TiO_2 on the performance of Pt/TiO_2 catalysts for furfural hydrogenation, RSC Adv. 12 (2022) 860–868.
[33] D. Rao, X. Xue, G. Cui, S. He, M. Xu, W. Bing, S. Shi, M. Wei, Metal-acid site synergistic catalysis in $Ru\text{-}ZrO_2$ toward selective hydrogenation of benzene to cyclohexene, Cayalysis Sci. Technol. 8 (2018) 236–243.
[34] M.D. Rhodes, A.T. Bell, The effects of zirconia morphology on methanol synthesis from CO and H_2 over Cu/ZrO_2 catalysts Part I. Steady-state studies, J. Catal. 233 (2005) 198–209.
[35] F. Su, Q. Wu, D. Song, X. Zhang, M. Wang, Y. Guo, Pore morphology-controlled preparation of ZrO_2-based hybrid catalysts functionalized by both organosilica moieties and Keggin-type heteropoly acid for the synthesis of levulinate esters, J. Mater. Chem. A 1 (2013) 13209–13221.
[36] J. Ni, W. Leng, J. Mao, J. Wang, J. Lin, D. Jiang, X. Li, Tuning electron density of metal nickel by support defects in Ni/ZrO_2 for selective hydrogenation of fatty acids to alkanes and alcohols, Appl. Catal. B: Environ. 253 (2019) 170–178.
[37] Y. Zhou, L. Liu, G. Li, C. Hu, Insights into the influence of ZrO_2 crystal structures on methyl laurate hydrogenation over Co/ZrO_2 catalysts, ACS Catal. 11 (2021) 7099–7113.
[38] G. Zhou, Y. Pei, Z. Jiang, K. Fan, M. Qiao, B. Sun, B. Zong, Doping effects of B in ZrO_2 on structural and catalytic properties of $Ru/B\text{-}ZrO_2$ catalysts for benzene partial hydrogenation, J. Catal. 311 (2014) 393–403.

[39] X. Si, J. Chen, Z. Wang, Y. Hu, Z. Ren, R. Lu, L. Liu, J. Zhang, L. Pan, R. Cai, F. Lu, Ni-catalyzed carbon-carbon bonds cleavage of mixed polyolefin plastics waste, J. Energy Chem. 85 (2023) 562–569.
[40] T. Zelenka, T. Horikawa, D.D. Do, Artifacts and misinterpretations in gas physisorption measurements and characterization of porous solids, Adv. Colloid Interface Sci. 311 (2023) 102831.
[41] M. Gao, J. Zhang, P. Zhu, X. Liu, Z. Zheng, Unveiling the origin of alkali metal promotion in CO_2 methanation over Ru/ZrO_2, Appl. Catal. B: Environ. 314 (2022) 121476.
[42] G. Zhou, X. Tan, Y. Pei, K. Fan, M. Qiao, B. Sun, B. Zong, Structural and catalytic properties of alkaline post-treated Ru/ZrO_2 catalysts for partial hydrogenation of benzene to cyclohexene, ChemCatChem 5 (2013) 2425–2435.
[43] J.L. Bi, Y.Y. Hong, C.C. Lee, C.T. Yeh, C.B. Wang, Novel zirconia-supported catalysts for low-temperature oxidative steam reforming of ethanol, Catal. Today 129 (2007) 322–329.
[44] T. Zhang, X. Ju, L. Liu, L. Liu, T. He, Y. Xu, H. Wang, P. Chen, Steering ammonia decomposition over Ru nanoparticles on ZrO_2 by enhancing metal–support interaction, Catal. Sci. Technol. 13 (2023) 5205–5213.
[45] Z. Wang, Y. Ma, J. Lin, Ruthenium catalyst supported on high-surface-area basic ZrO_2 for ammonia synthesis, J. Mol. Catal. A: Chem. 378 (2013) 307–313.
[46] M.G. Cattania, F. Parmigiani, V. Ragaini, A study of ruthenium catalysts on oxide supports, Surf. Sci. 211-212 (1989) 1097–1105.
[47] L.M.N.C. Alves, M.P. Almeida, M. Ayala, C.D. Watson, G. Jacobs, R.C. Rabelo-Neto, F.B. Noronha, L.V. Mattos, CO_2 methanation over metal catalysts supported on ZrO_2: Effect of the nature of the metallic phase on catalytic performance, Chem. Eng. Sci. 239 (2021) 116604.
[48] W. Yan, B. Jin, J. Cheng, X. Shi, H. Zhong, F. Jin, Ru/ZrO_2 as a facile and efficient heterogeneous catalyst for the catalytic hydrogenation of bicarbonate using biodiesel-waste glycerol as a hydrogen donor, ACS Sustain. Chem. Eng. 10 (2022) 5374–5383.
[49] Y. Xin, Z. Zheng, Z. Luo, C. Jiang, S. Gao, Z. Wang, C. Zhao, The influence of pore structures and Lewis acid sites on selective hydrogenolysis of guaiacol to benzene over Ru/TS-1, Green. Energy Environ. 7 (2022) 1014–1023.
[50] T. Nozawa, Y. Mizukoshi, A. Yoshida, S. Naito, Aqueous phase reforming of ethanol and acetic acid over TiO_2 supported Ru catalysts, Appl. Catal. B: Environ. 146 (2014) 221–226.
[51] F. Han, H. Liu, W. Cheng, Q. Xu, Highly selective conversion of CO_2 to methanol on the $CuZnO\text{-}ZrO_2$ solid solution with the assistance of plasma, RSC Adv. 10 (2020) 33620–33627.
[52] L. Chen, Y. Li, X. Zhang, Q. Zhang, T. Wang, L. Ma, Mechanistic insights into the effects of support on the reaction pathway for aqueous-phase hydrogenation of carboxylic acid over the supported Ru catalysts, Appl. Catal. A: Gen. 478 (2014) 117–128.
[53] A. Bernas, N. Kumar, P. Laukkanen, J. Väyrynen, T. Salmi, D.Y. Murzin, Influence of ruthenium precursor on catalytic activity of Ru/Al_2O_3 catalyst in selective isomerization of linoleic acid to cis-9, trans-11- and trans-10, cis-12-conjugated linoleic acid, Appl. Catal. A: Gen. 267 (2004) 121–133.